REVIEW

Review of Methods for Texture Analysis of Myocardium From Echocardiographic Images: A Means of Tissue Characterization

Edmund Kenneth Kerut, M.D.,*† Michael Given, Ph.D.,* and Thomas D. Giles, M.D.*

*Cardiovascular Research Laboratory, LSU Health Sciences Center, New Orleans, Louisiana, and †Heart Clinic of Louisiana, Marrero, Louisiana

This review discusses the definition of texture and identifies its utility in echocardiography for characterization of tissue. Methods used for quantification of texture in echocardiography and other disciplines are discussed. Several methodologies, particularly the wavelet method of texture quantification, seem to be promising. Image texture analysis appears to be a fertile area for research in echocardiography. (ECHOCARDIOGRAPHY, Volume 20, November 2003)

texture, *wavelet*, *echocardiography*, *fractal*, *statistical*, *cooccurrence*

Early detection and quantitative assessment of tissue alteration in a disease process is a challenge for noninvasive imaging techniques. Direct histologic assessment is limited by a requirement for obtaining tissue for examination. Therefore, to better characterize the onset and progression of myocardial disease, a noninvasive imaging technique for distinguishing normal from abnormal tissue would be of particular importance.

Tissue characterization by ultrasound utilizes information derived from the interaction of ultrasound waves with tissue. Diffuse scattering occurs when ultrasound interacts with tissue interfaces where the structures are usually smaller than the wavelength of the ultrasound signal. Small changes in acoustic impedance of interfaces within the tissue produce this diffuse scattering. Most of the ultrasound energy is directed away (scattered) from the beam and only a small fraction of the original energy is reflected back towards the transducer. In contradistinction to specular reflectors (bright boundary interfaces between structures), diffuse scattering is usually independent of the ultrasound incident angle. Rayleigh scattering is a form of diffuse scattering, but occurs from interfaces much smaller than the ultrasound wavelength. Defined as ultrasound speckle, both diffuse and Rayleigh scattering are important in generating the appearance of tissue texture.

The characterization of myocardial tissue by ultrasound was attempted in 1957, using excised human hearts to distinguish infarcted from normal myocardium.[1] Echocardiographic methods to characterize myocardium have included quantitative estimates of frequency-dependent myocardial attenuation,[2] and have been subsequently used to distinguish normal from abnormal myocardium.[3–6]

Texture

Texture analysis is an approach to tissue characterization based on the spatial distribution of ultrasound amplitude signals within a region of interest (ROI). Although texture is a characteristic of image analysis in many disciplines, a formal definition does not exist. The term texture may be considered as:

> "an attribute representing the spatial arrangement of the gray levels of the pixels in a region"[7]

Address for correspondence and reprint requests: Edmund Kenneth Kerut, M.D., Heart Clinic of Louisiana, 1111 Medical Center Blvd, Suite N613, Marrero, LA 70072; Fax: (504) 349-6621; E-mail: kenkerut@pol.net

> "We intuitively view this descriptor as providing a measure of properties such as smoothness, coarseness, and regularity."[8]

> "Image texture can be qualitatively evaluated as having one or more of the properties of fineness, coarseness, smoothness, granulation, randomness, lineation, or being motled, irregular, or hummocky. Each of these adjectives translates into some property of the tonal primitives and the spatial interaction between the tonal primitives."[9]

Skorton et al.[10] defined echocardiographic image texture as:

> "the two-dimensional spatial distribution of echocardiographic amplitudes or gray levels."

Subjective assessment of tissue parenchyma is clinically possible for characterizing tissue, even though the ultrasound image visualized on the cathode ray tube (CRT) is smoothed and nonlinearly processed. For example, echocardiographers qualitatively describe fibrosis, amyloid "sparkling," and textural changes of the interventricular septum in hypertrophic cardiomyopathy, demonstrating a potential benefit for quantitative texture analysis.

Although echocardiographic myocardial speckle is dependent upon the ultrasound instrument and transducer, it is also influenced by alterations in tissue pathology. Microscopic structural changes affect myocardial texture (speckle), hence, echocardiographic texture (Fig. 1) does contain tissue structure related information.[10–12] Attempts to numerically quantify image texture have been somewhat problematic.

Qualitative Assessment of Texture

In 1983, Bhandari and Nanda[13] described a qualitative approach to texture patterns of myocardium based on visual inspection of videotaped two-dimensional echocardiograms from patients with a variety of disorders. They proposed a classification system based on the textural patterns visualized as: type I (uniform, low intensity, fine speckle: normal), type IIA (multiple, discrete, 3 to 5 mm, bright echoes in all walls), type IIB (one or more, but not all, walls with type IIA pattern), and type IIC (uniform

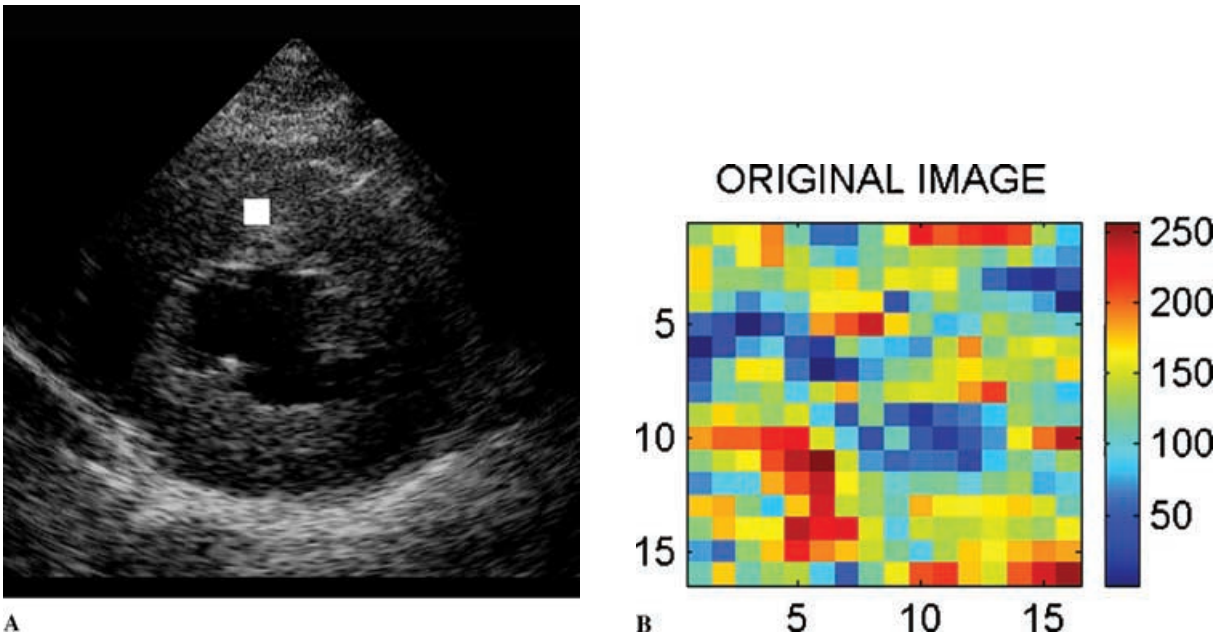

Figure 1. *Parasternal short-axis view (end-diastolic frame) of a human patient with hypertension. In this example the transducer is a 3.0-MHz probe with a depth setting of 15 cm. The images in RGB format were unprocessed (no temporal or spatial smoothing, or logarithmic compression) and converted to 8-bit grayscale. A 16 × 16 pixel region of interest (ROI) has been "extracted" from the anteroseptum (left panel), and saved for offline analysis. Color scale representation (right panel) of the 16 × 16 pixel ROI. This map artificially assigns a wide range color scale to a range of gray scale values in order to visually highlight subtle differences in intensity values between pixels.*

very bright echoes in one wall or region). This approach is useful, but lacks specificity.

Quantitative Assessment of Texture

Statistical Techniques

Characterization of tissue texture using statistical techniques (Appendix 1) for analysis of ultrasound scatter has been performed to identify various cardiomyopathic abnormalities. These include experimental myocardial contusion,[14] amyloid infiltration,[15] amyloid and hypertrophic cardiomyopathy,[16] coronary ischemia,[17] myocardial nonviability,[18] transplant rejection,[19] and myocarditis.[20] These reports used first order gray level histogram statistics for evaluation (usually 8-bit information), including mean gray scale, standard deviation of the mean, skewness (deviation of the pixel distribution from a symmetrical shape), and the kurtosis (steepness of the pixel distribution). Second order statistical methods[14–16,20] typically utilized gray-level run-length measures and the gray level cooccurence matrix (Appendix 1), however the use of second-order statistics as sufficient for texture analysis has been questioned.[21] Recently, myocardial texture was quantified by contrast echocardiography in a canine model of myocardial infarction using second order statistics. Entropy calculations (average and maximal) were applied from a cooccurrence matrix analysis of a ROI to discern viable from nonviable myocardium.[22] Statistical methods to quantitate texture were also recently utilized in a canine model using contrast echocardiography to discern perfused from nonperfused myocardium.[23]

The above described statistical methods used for quantitation of myocardial texture may have limited capability. Analysis was limited in many studies because they were performed using digitized video signals, introducing more noise into the image. As first order statistical methods do not take into account the spatial distribution of pixels, this method may be problematic for texture quantification. The ROI is relatively small (often $\sim 16 \times 16$ pixel matrix) in order to avoid specular reflections (endocardial and epicardial borders). A small ROI limits the capability of first and second order statistical methodologies.

Fractal Techniques

The fractal concept as developed by Mandelbrot[24] provides a means to explain the "ruggedness" of surfaces and may be applied to image analysis because images may be viewed as surfaces (Appendix 1). Medical images demonstrate a certain degree of self-similarity over a range of scales, lending to development of algorithms for fractal analysis of these images.[25,26]

Frequency Domain (Fourier Analysis)

Limited work exists in the area of quantifying medical ultrasound image texture using frequency transform techniques. Methods include the Wigner distribution,[27] autoregressive techniques,[28] and the Fourier transform[29,30] to estimate the power spectral density (PSD) of the image. The Discrete Fourier Transform (DFT) is usually used for performing the Fourier transform on a computer. The Fourier transform of an image is plotted as a power spectral density plot, with the horizontal axis representing image frequency, and the vertical axis as magnitude. Any periodic structure occurring in the original image will have a frequency peak in the PSD. In the center of a PSD plot is frequency zero (DC component), and extending radially outward is increasing frequency. These peaks on the PSD will have a "noisy" background, corresponding to nonperiodic information, along with noise and textural information. If one plots the radial decrease of the PSD magnitude as a log-log plot, the slope serves as a measure of image "roughness" and hence texture.[31,32]

Wavelet Techniques

A mathematical tool for signal processing termed wavelet analysis (Appendix 1) has been introduced recently as a way to look at a signal at different resolutions.[33–36] Mallat[37,38] developed the dyadic wavelet method of multiresolution analysis, particularly useful for image processing. In effect this method decomposes a signal into a set of approximation coefficients (low frequency components) and the remainder as the detail coefficients (high frequency components). The approximation coefficients can be successively decomposed into multilevel approximation coefficients and their corresponding detail coefficients. When one is analyzing a two-dimensional signal, such as an image, at each level of decomposition there are three sets of generated detail coefficients: horizontal (vertical edge), vertical (horizontal edge), and diagonal.

The approximation coefficients are often utilized for image compression, and the detail

coefficients are generally discarded.[39–41] These detail coefficients contain noise and artifact, but also contain textural information.[42] The generated detail coefficients have been used to quantify the texture of various surfaces,[42] in satellite remote sensing,[43] and for characterization of fat content and marbling in beef cattle muscle.[44]

Recently, investigators used the Haar wavelet transform with an image extension method and wavelet decomposition to calculate texture energy and differentiate viable from nonviable myocardium.[45,46] The term "energy" has been borrowed from physics and is defined as the sum of the squares of the coefficient values. Wavelets compress most of the energy from the original signal into the approximation coefficients. Wavelets conserve energy, meaning that the sum of the energy from the approximation coefficients and detail coefficients equals the energy of the original signal. In image compression, the more energy conserved into the approximation coefficients, the better the compression achieved. The Haar wavelet stores more energy in the detail coefficients than many other wavelet forms and is, therefore, potentially better suited for image texture analysis.

Our laboratory used the two-dimensional Haar dyadic wavelet decomposition method to calculate myocardial textural energy in alcoholic and diabetic rat models of cardiomyopathy. Texture energy calculations of myocardium detected alterations in both models by 5 weeks of disease, whereas M-mode echocardiographic changes were not noted until 10 weeks.[47] Detail coefficients have been used by investigators with other than the Haar wavelet to characterize various surfaces.[48] Also, a vector of features from first and second order (cooccurrence matrix) statistics has been used to classify textures of surfaces.[49–51] In addition, textural features have been used in a neural network scheme to classify clouds from satellite imagery.[52]

By performing wavelet decomposition repeatedly to obtain multiple levels of detail coefficients, and then performing energy and statistical measures on these multiple layers of coefficients, it may be possible to further improve textural discrimination. Furthermore, there is a theoretical possibility of enhanced quantification of tissue texture of ultrasound images using higher order harmonics. Higher frequencies with less near field artifact are present with harmonic imaging. As Doppler tissue imaging represents tissue motion, this methodology would not be useful for analysis of tissue texture.

Conclusions

This review discusses the definition of image texture and its application to echocardiography as a method of tissue characterization. Other methods for quantitation of texture, applied in other disciplines, are also discussed. With ultrasound, several methodologies, particularly the wavelet method of texture quantification, seem to be promising. Image texture analysis appears to be a fertile area for research in echocardiography.

APPENDIX

First and Second Order Statistics

Quantitative myocardial image texture analysis using statistical methods has been performed mostly using gray level histogram statistics (first order statistics), and also gray level run-length and gray level difference statistics (second order).

First order statistics include the grayscale histogram mean (average intensity of the ROI), standard deviation (σ) and variance (σ^2; variance is the square value of standard deviation), skewness, and kurtosis.

Whereas the mean is the first moment, o^2 is the second moment. Another second moment measure is the relative smoothness (RS), defined as:

$$RS = 1 - [1/(1 + \sigma^2)]$$

RS is valued 0 for a constant intensity, and approaches 1 for an increasing variance of ROI pixel intensities. Skewness (third moment) is the degree of asymmetry of a distribution, or deviation of the pixel distribution from a symmetrical shape. If a distribution has a longer "tail" to the right of a central maximum, then the distribution is skewed to the right, and has positive skewness. For the reverse, the distribution is skewed to the left, and has negative skewness. There is no completely accepted method to measure skewness (Sk), but it may be defined as:

$$Sk = (1/N) \sum [(x - mean)/o]^3$$

where N is the number of pixels, and mean is the ROI average intensity.

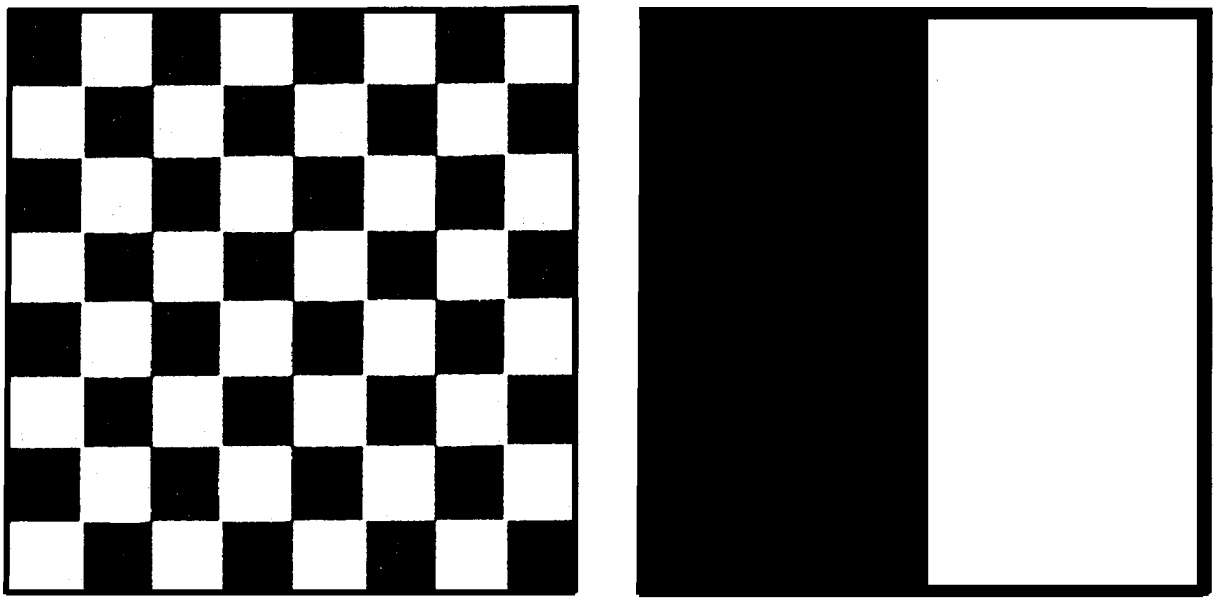

Figure 2. *Illustration of two very different regions of interest (ROI) with two different textures, but with identical first order statistics: the left panel appears as a chessboard, and the right panel has the same number of black and white squares, but they appear completely different. The histograms of both ROI are the same; hence, the mean, standard deviation, skewness, and kurtosis are the same. This example demonstrates that first order statistics contain no information about the relative position of pixels in relation to each other.*

Kurtosis (fourth moment) is the degree of steepness of the pixel distribution. If a distribution has a high peak, it is leptokurtic, whereas a flattened peak is platykurtic.

Kurtosis (Kur) may be defined as:

$$\text{Kur} = (1/\text{N}) \sum [(\text{x} - \text{mean})/\sigma]^4 - 3$$

First order statistics, especially the mean of the intensity, are poor measures of texture. Two different ROIs may have identical statistics, but the pixels may have very different spatial relationships (Fig. 2).

With gray level run-length statistics, a gray level run is a set of consecutive pixels that have the same gray level value (or value within a range). The length is the number of pixels occurring before there is a change in value. This approach identifies coarse textures as having many pixels in a run, and fine textures as having few pixels in a run. With this method, one could calculate five features in each of four directions (0-, 45-, 90-, and 135-degree direction) from each pixel, as each pixel is sequentially evaluated within a ROI. These run-length features include short run emphasis, long run emphasis, gray level nonuniformity, run length nonuniformity, and fraction of image in runs.[9] ROI run-length features are generally measures of gray level heterogeneity and the size of ultrasound reflections. A ROI with large ultrasound reflections will have long run-lengths, and likewise relatively small echo reflections will have short run-lengths. Nonuniformity features are representative of the homogeneity of the echo reflectors within the ROI.

Gray level difference features are indicative of ROI heterogeneity, and are calculated by measuring the difference in gray level value between pixels that are separated by various distances in different directions (usually in 45-degree intervals, thus in eight directions). Gray level difference features are usually expressed in the form of a generated cooccurrence matrix from the ROI.[9] A cooccurrence matrix may be generated as follows:

(1) Consider an image ROI having multiple gray level values, and reduce the number (usually 32 or 64 levels) to n.

(2) Let A be a (n $\times$ n) matrix, where n is an integer, whose element a(i, j) is the number of times that a pixel with gray level g(1) occurs

(in a position as specified by a position operator) relative to points with a gray level g(1) to g(k). Note that the size of the matrix is determined by the number of gray levels in the image ROI.

For example, consider an image ROI with only three gray levels, where g(1) = 0, g(2) = 1, and g(3) = 2. The position operator for this example will be defined as "one pixel down and one to the right." If an image ROI (size 5 × 5) has the following values:

$$\begin{matrix} 1 & 2 & 1 & 0 & 1 \\ 2 & 1 & 0 & 1 & 1 \\ 1 & 2 & 1 & 0 & 2 \\ 0 & 1 & 1 & 1 & 0 \\ 2 & 1 & 0 & 0 & 1 \end{matrix}$$

then the generated matrix is:

$$A = \begin{matrix} 2 & 2 & 0 \\ 2 & 5 & 1 \\ 1 & 1 & 1 \end{matrix}$$

In this matrix a(1, 1), the top left number in matrix A, is the number of times that a pixel in the image ROI with value 0 has a pixel one down and one to the right with a value of 0. Likewise, a(1, 2) is the number of times that a pixel in the image ROI with value 0 has a pixel one down and one to the right with a value of 1. The entire matrix is then generated. If one adds up all the values of the matrix (15 in this example) and divides each value in the matrix by this matrix, the resultant is the cooccurrence matrix. The cooccurrence matrix in the above example was generated by looking one unit "down and to the right" of the reference pixel. Eight matrices may be generated performing a similar procedure at 45-degree increments. In evaluation of echocardiographic images, deciding how many pixels away from the reference pixel to use (reference distance) is difficult, and is probably dependent on speckle size.

When forming cooccurrence matrices from an image ROI, generated data may become much larger than the size of the original ROI. Therefore, various features of each cooccurrence matrix are usually calculated, and these features are then used to characterize a ROIs texture. Commonly calculated co-occurrence matrix features, from more than twenty, include the mean, standard deviation, entropy, maximum probability, contrast, inverse difference moment, correlation,[9] and kappa for texture periodicity.[53]

From these computed features, one may teach a computer program to learn to differentiate textures. An unknown texture ROI may then be "fed" into the computer, and the computer will determine how close the unknown texture features are to those already in it's memory. A difficulty with statistical methodologies (first and second order) is that results will change with alterations in ultrasound power and gain settings.

Fractals and Texture

> "A fractal is a geometrical figure that consists of an identical motif repeating itself on an ever-reduced scale."[54]

A fractal object has features over a range of scales. As its dimension (length, area, volume, and higher dimensions) is viewed at higher resolutions, further finer features are noted. The size of a nonfractal's smallest feature is its characteristic scale. Characteristics of fractals include that of self-similarity at various resolutions, scaling (the measured length of an object increases as measurements are made at finer resolutions), dimension (a measure of self-similarity and scaling), and statistical properties.

Geometrical self-similarity means that an object is self-similar exactly at differing resolutions. Fractal biologic objects, however, have statistical self-similarity. Different scales of an object are not exactly the same, but the number of pieces of each size making up the object is called the probability density function, and is similar at different resolutions.

The length of an object is proportional to its length at other scales, by a constant of proportionality. Length, area, or volume measurement will be dependent on the resolution level used. How this measurement is dependent on the scale is termed the scaling relationship. The Power law for a fractal object states that the logarithm of the measurement (length, area, volume) plotted against the logarithm of the scale is a straight line. This relationship was first noted by Lewis Fry Richardson, and published after his death. In 1961, Mandelbrot found in Richardson's work that measurements of the length of variously selected coastlines were dependent in a logarithmic fashion, on the scale of a map used (Fig. 3). As the scale of the coastline increases, so does the coastline get longer.[55]

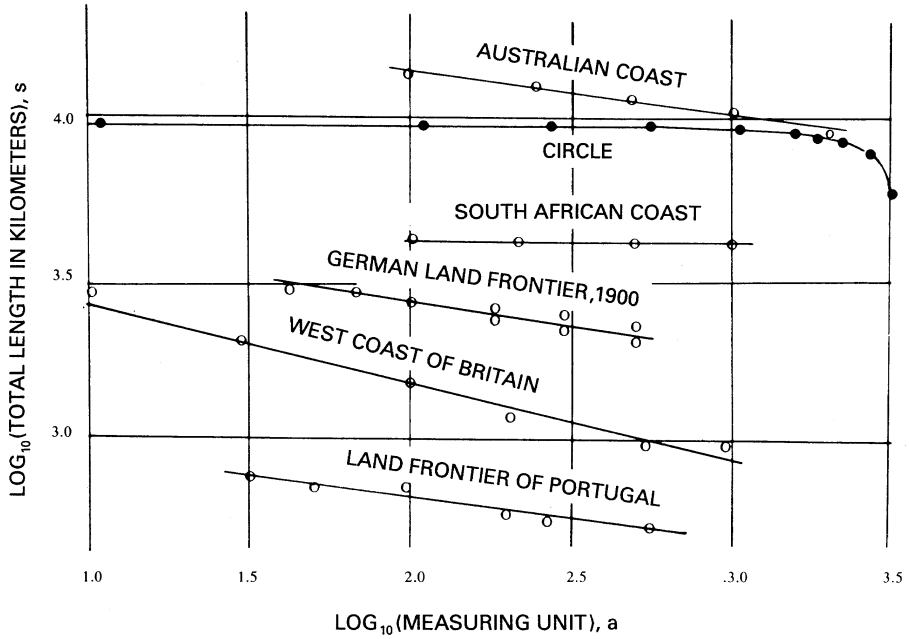

Figure 3. *Results of Richardson's measurements of various European coastlines. The log-log relationship is linear for a fractal structure. The x-axis is the measuring unit used (kilometers in this example), and the y-axis is the total length, area, or volume (length in kilometers in this example). Note that the slope of a circle (nonfractal) is zero over a wide range and becomes nonlinear (see text).*

Mandelbrot used the term fractal from the fact that a fractal is fragmented into increasingly finer pieces and has a fractional dimension.

The fractal dimension provides a measure of the fractal properties of self-similarity and scaling, and says how many extra pieces of an object are found when increased to a higher resolution. For biologic images and objects, the fractal dimension is often determined by the scaling relationship. The slope of the line for the west coast of Britain (Fig. 3) is about 0.22, and is known as the Hurst coefficient.[56] Mandelbrot termed the fractal dimension as 1 added to the slope of the generated line, therefore its fractal dimension is 1.22.

Wavelet Analysis

By definition, a wavelet (localized wavelike function) is a waveform of limited duration that has an average value of zero. Whereas Fourier analysis assumes a signal to be infinitely long and each frequency is defined for an infinite sine wave, the wavelet transform breaks up a signal into shifted (translation) and scaled (stretching or compressing) versions of a mother wavelet signal. A wavelet may assume one of many shapes, but it must be a finite signal and have an average value of zero. Wavelets are better suited to analyze finite, discontinuous, and statistically nonstationary signals.[33–36] Wavelets decompose a discrete signal into two subsignals, each of half the original signal's length. In effect, one subsignal is a moving average (trend), and the other is a moving difference (fluctuation).

A continuous (integral) wavelet transform (CWT) is the sum over the duration of the signal multiplied by shifted and scaled versions of the wavelet function. The results of the CWT are wavelet coefficients, which are a function of scale and position. The higher the values of the coefficients, the more similar the wavelet is to the original signal.

The discrete wavelet transform (DWT) uses only powers of two (dyadic) for shifting and scaling wavelets. With the DWT one obtains a running trend subsignal or what is termed approximation coefficients (low-pass frequency and high scale components). The other subsignal is a running difference or what is termed detail coefficients (high-pass frequency and low scale components). The sum of the number of approximation coefficients and detail coefficients is that of the number of points (pixels in an image) in the original signal.

One-dimensional wavelets are used in analysis of various time domain signals including evoked potentials,[57] heart rate variability analysis,[58] and ventricular late potentials.[59,60] Two-dimensional wavelets have been used for image compression. Theoretically, higher order data (volumes or time varying images) may be analyzed with higher order dimension wavelets. When analyzing a two-dimensional signal, at each level of decomposition there are three sets of detail coefficients generated, horizontal (vertical edge), vertical (horizontal edge), and diagonal.

The process of forming the approximation and detail coefficients from the original signal is termed wavelet decomposition. The Haar wavelet (also termed Daubechies db1) is the simplest type of wavelet resembling a step function. With the Haar wavelet, the approximation coefficients are generated by first taking the average of the first pair of signal values and multiplying it by the square root of 2. This yields the first approximation coefficient. Similarly, the second approximation coefficient is generated by taking the next pair (third and fourth values) of signal values and taking its average and multiplying it by the square root of 2. This continues until the entire signal has been decomposed. The detail coefficients are obtained by subtracting the second from the first signal value, and then multiplying it by the square root of 2. The entire signal is evaluated in a similar manner.

For many applications (signal and image compression), the approximation coefficients are most important, whereas the detail coefficients contain noise and artifact, but also contain textural information. As mentioned earlier, the approximation coefficients may be further resolved into a second level set of approximation and detail coefficients. This process may theoretically continue until only a single value for the approximation and detail coefficients remain, but usually there is no information gained by decomposing a signal that far (Fig. 4).

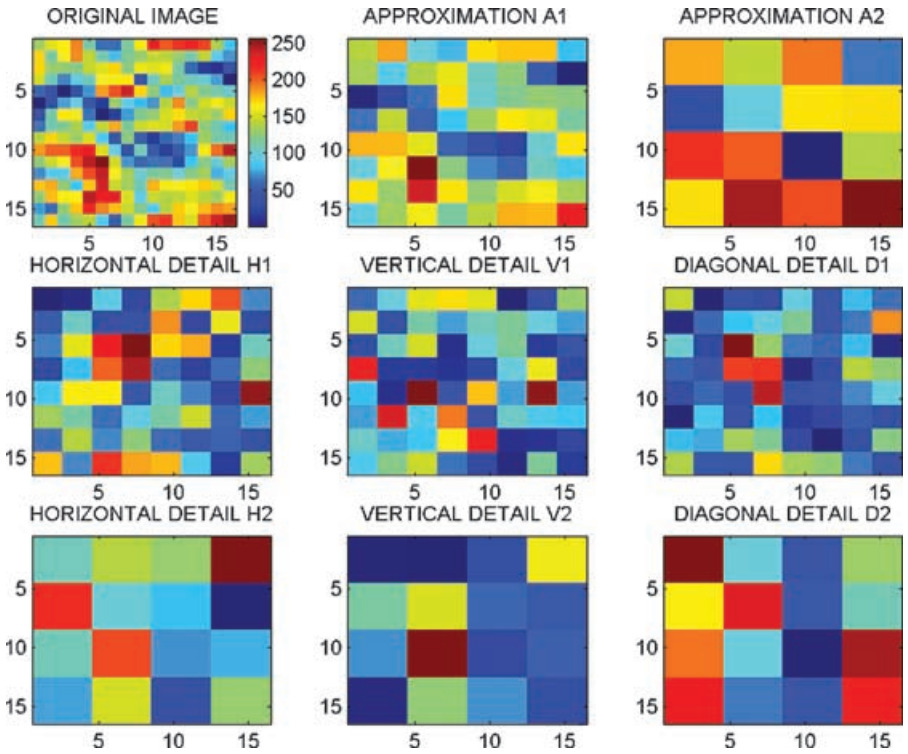

Figure 4. *Color scale representation of a gray scale image (original image) of a 16 × 16 pixel region of interest (ROI) from Figure 1. Wavelet image decomposition using the Haar wavelet transform yields a first level approximation image (A1), and first level detail images horizontal (H1), vertical (V1), and diagonal (D1). Decomposition of (A1) likewise yields a second level approximation image (A2), and second level detail images horizontal (H2), vertical (V2), and diagonal (D2).*

References

1. Wild JJ, Crafford HD, Reid JM: Visualization of the excised human heart by means of reflected ultrasound or echography. *Am Heart J* 1957;54:903–906.
2. Miller JG, Perez JE, Sobel BE: Ultrasonic characterization of myocardium. *Prog Cardiovasc Dis* 1985;28:85–110.
3. Haskell WL, Masuyama T, Nellessen U, et al: Serial measurements of integrated ultrasonic backscatter in human cardiac allografts for the recognition of acute rejection. *Circulation* 1990;81:829–839.
4. Sagar KB, Rhyne TL, Pelc LR, et al: Intramyocardial variability in integrated backscatter: Effects of coronary occlusion and reperfusion. *Circulation* 1987;75:436–442.
5. Sagar KB, Pelc LR, Rhyne TL, et al: Role of ultrasonic tissue characterization to distinguish reversible from irreversible myocardial injury. *J Am Soc Echocardiogr* 1990;3:471–477.
6. Wickline SA, Thomas JL III, Miller JG, et al: Sensitive detection of the effects of reperfusion on myocardium by ultrasonic tissue characterization with integrated backscatter. *Circulation* 1986;74:389–400.
7. IEEE: *Standard Glossary of Image Processing and Pattern Recognition Terminology.* Piscataway, NJ: IEEE Press, 1990.
8. Gonzales RC, Woods RE: *Digital Image Processing.* Reading, MA: Addison-Wesley Publishing Company, 1992, p. 508.
9. Haralick RM: Statistical and structural approaches to texture. *Proc IEEE* 1979;67:786–804.
10. Skorton DJ, Collins SM, Woskoff SD, et al: Range- and azimuth-dependent variability of image texture in two-dimensional echocardiograms. *Circulation* 1983;68:834–840.
11. Wagner RF, Smith SF, Sandrick JM, et al: Statistics of speckle in ultrasound B-scans. *IEEE Trans Sonics Ultrason* 1983;SU-30:156.
12. Smith SW, Wagner RF: Ultrasound speckle size and lesion signal to noise ratio: Verification of theory. *Ultrason Imaging* 1994;6:174.
13. Bhandari AK, Nanda NC: Myocardial texture characterization by two-dimensional echocardiography. *Am J Cardiol* 1983;51:817.
14. Skorton DJ, Collins SM, Nichols J, et al: Quantitative texture analysis in two-dimensional echocardiography: Application to the diagnosis of experimental myocardial contusion. *Circulation* 1983;68:217–223.
15. Pinamonti B, Picano E, Ferdeghini EM, et al: Quantitative texture analysis in two-dimensional echocardiography: Application to the diagnosis of myocardial amyloidosis. *J Am Coll Cardiol* 1989;14:666–671.
16. Chandrasekaran K, Aylward PE, Fleagle SR, et al: Feasibility of identifying amyloid and hypertrophic cardiomyopathy with the use of computerized quantitative texture analysis of clinical echocardiographic data. *J Am Coll Cardiol* 1989;13:832–840.
17. Picano E, Faletra F, Marini C, et al: Increased echo density of transiently asynergic myocardium in humans: A novel echocardiographic sign of myocardial ischemia. *J Am Coll Cardiol* 1993;21:199–207.
18. Marini C, Picano E, Varga A, et al: Cyclic variation in myocardial gray level as a marker of viability in man: A videodensitometric study. *Eur Heart J* 1996;17:472–479.
19. Stempfle H, Angermann CE, Kraml P, et al: Serial changes during acute cardiac allograft rejection: Quantitative ultrasound tissue analysis versus myocardial histologic findings. *J Am Coll Cardiol* 1993;22:310–317.
20. Ferdeghini EM, Pinamonti B, Picano E, et al: Quantitative texture analysis in echocardiography: Application to the diagnosis of myocarditis. *J Clin Ultrasound* 1991;19:263–270.
21. Gagalowicz A: A new method for texture field synthesis: Some applications to the study of human vision. *IEEE Trans Pattern Anal Machine Intell* 1982;PAMI-3:520–533.
22. Ohmori K, Cotter B, Leistad E, et al: Assessment of myocardial postreperfusion viability by intravenous myocardial contrast echocardiography: Analysis of the intensity and texture of opacification. *Circulation* 2001;103:2021–2027.
23. Bae RY, Belohlavek M, Greenleaf JF, et al: Myocardial contrast echocardiography: Texture analysis for identification of nonperfused versus perfused myocardium. *Echocardiography* 2001;18:665–672.
24. Mandelbrot BB: *The Fractal Geometry of Nature.* San Francisco: Freeman, 1983.
25. Chen CC, Daponte JS, Fox MD: Fractal feature analysis and classification in medical imaging. *IEEE Trans Med Imaging*1989;8:133–142.
26. Kuklinski WS: Utilization of fractal image models in medical image processing. *Fractals* 1994;2:363–369.
27. Cristobal G, Bescos J, Santamaria J: Image analysis through the Wigner distribution function. *Appl Optics* 1989;28:262–271.
28. Kartikeyan B, Sarkar A: An identification approach for 2-D autoregressive models in describing textures. *CVGIP: Graphical Models Image Process* 1991;53:121–131.
29. Bajcsy R, Lieberman L: Texture gradient as a depth cue. *Comput Graphics Image Process* 1976;5:52–67.
30. Day DD, Rogers D: Fourier-based texture measures with application to the analysis of the cell Structure of baked products. *Digital Signal Process* 1996;6:138–144.
31. Mitchell MW, Bonnell DA: Quantitative topographic analysis of fractal surfaces by scanning tunneling microscopy. *J Mat Res* 1990;5:224–225.
32. Russ JC: Surface characterization: Fractal dimensions, Hurst coefficients and frequency transforms. *J Comput Assist Microsci* 1990;2:161–184.
33. Aldroubi A: The wavelet transform: A surfing guide. InAldroubi A, Unser M (eds): *Wavelets in Medicine and Biology.* New York: CRC Press, 1996, pp 3–36.
34. Daubechies I: *Ten Lectures on Wavelets.* Philadelphia: Society for Industrial and Applied Mathematics, 1992.
35. Teolis A: *Computational Signal Processing With Wavelets.* Boston: Birkhauser, 1998, pp 59–78.
36. Unser M: A practical guide to the implementation of the wavelet transform. InAldroubi A, Unser M (eds): *Wavelets in Medicine and Biology.* New York: CRC Press, 1996, pp 37–73.
37. Mallat S: A theory for multiresolution signal decomposition: The wavelet representation. *IEEE Trans Pattern Anal Mach Intell* 1989;11:674–693.
38. Mallat S: Multifrequency channel decomposition of images and wavelet models. *IEEE Trans Acoust Speech Signal Process* 1989;37:2091–2110.
39. Chui CK: *Wavelets: A Mathematical Tool for Signal Analysis.* Philadelphia: Society for Industrial and Applied Mathematics, 1997, pp 178–180.

40. Press WH, Teukolsky SA, Vetterling WT, et al: *Numerical Recipes in FORTRAN: The Art of Scientific Computing.* (Second edition) New York: Cambridge University Press, 1992, pp 596–597.
41. Wickerhauser MV: *Adopted Wavelet Analysis From Theory to Software.* Wellesley, MA: AK Peters, 1994, pp 361–377.
42. Prasad L, Lyengar SS: *Wavelet Analysis With Applications to Image Processing.* Boca Raton, FL: CRC Press, 1997, pp 235–239, 258–262.
43. Mecocci A, Gamba P, Marazzi A, et al: Texture segmentation in remote sensing images by means of packet wavelets and fuzzy clustering. *Int Soc Optical Eng Synth Aperture Radar Pass Micro Sens* 1995;2584:142–151.
44. Kim ND, Main V, Wilson D, et al: Ultrasound image texture analysis for characterizing intramuscular fat content of live beef cattle. *Ultrason Imaging* 1998;20:191–205.
45. Mojsilovic A, Popovic MV, Neskovic AN, et al: Wavelet image extension for analysis and classification of infarcted myocardial tissue. *IEEE Trans Biomed Eng* 1997;44:856–866.
46. Neskovic AN, Mojsilovic A, Jovanovic T, et al: Myocardial tissue characterization after acute myocardial infarction with wavelet image decomposition: A novel approach for the detection of myocardial viability in the early post infarction period. *Circulation* 1998;98:634–641.
47. Kerut EK, Given MB, McIlwain E, et al: Echocardiographic texture analysis using the wavelet transform: Differentiation of early heart muscle disease. *Ultrasound Med Biol* 2000;26:1445–1453.
48. Carter PH: Texture discrimination using wavelets. *SPIE: Application Digital Image Proc XIV* 1991;1567:432–438.
49. Van de Wouwer G, Scheunders P, Van Dyck D: Statistical texture characterization from discrete wavelet representations. *IEEE Trans Image Proc* 1999;8:592–598.
50. Scheunders P, Livens S, Van de Wouwer G, et al: *Wavelet-Based Texture Analysis.* Antwerpen, Belgium: Vision Lab, Department of Physics, University of Antwerp, 1997.
51. Van de Wouwer G: *Wavelets for Multiscale Texture Analysis.* PhD thesis. Antwerpen, Belgium: Department of Physics, University of Antwerp, 1998.
52. Tian B, Shaikh MA, Azimi-Sadjadi MR, et al: A study of cloud classification with neural networks using spectral and textural features. *IEEE Trans Neural Networks* 1999;10:138–151.
53. Parkinnen J, Selkinaho K, Oja E: Detecting texture periodicity from the cooccurrence matrix. *Pattern Recog Lett* 1990;11:43–50.
54. Lauwerier H: Fractals: *Endlessly Repeated Geometrical Figures.* Princeton, NJ: Princeton University Press, 1991, p 1.
55. Richardson LF: The problem of contiguity: An appendix to statistics of deadly quarrels. *Gen System Yearbook* 1961;6:139–187.
56. Russ JC: Surface characterization: Fractal dimensions, Hurst coefficients, and frequency transforms. *J Comput Assist Microsc* 1990;2:249–257.
57. Bertrand O, Bohorquez J, Pernier J: Time-frequency digital filtering based on an invertible wavelet transform: an application of evoked potentials. *IEEE Trans Biomed Eng* 1994;41:77–88.
58. Gamero LG, Risk M, Sobh JF, et al: Heart rate variability analysis using waelet transform. *IEEE Comput Cardiol* 1996;23:177–180.
59. Batista A, English M: A multiresolution wavelet method for characterization of ventricular late potentials. *IEEE Comput Cardiol* 1996;23:625–628.
60. Meste O, Rix H, Caminal P, et al: Ventricular late potentials characterization in time-frequency domain by means of a wavelet transform. *IEEE Trans Biomed Eng* 1994;41:625–634.